TECHNICAL RESEARCH REPORT

SYSTEMS RESEARCH CENTER

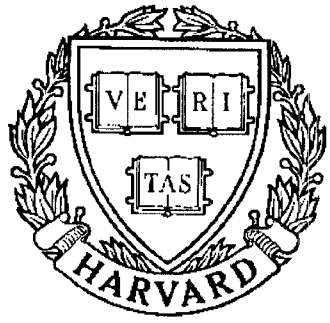

Supported by the National Science Foundation Engineering Research Center Program (NSFD CD 8803012), the University of Maryland, Harvard University, and Industry

An Integrated Approach to Calibrate an Untended Machining System

by J.E. Parker, G.M. Zhang, J.A. Kirk and D.K. Anand

TR 91-60

An Integrated Approach to Calibrate an Untended Machining System

J.E. Parker, G.M. Zhang, J.A. Kirk and D.K. Anand

Department of Mechanical Engineering and Systems Research Center
University of Maryland
College Park, MD 20742

Abstract

This paper presents a new methodology for the calibration of an untended machining system. The methodology requires the calibration conducted under both static and dynamic loading conditions. The transformation matrix method was used to establish the mapping function between the performance measure of interest (input) and the control signal (output). A prototype system, building on an CNC machining center equipped with a magnetic spindle, was developed to demonstrate a strategy for monitoring the tool wear progress through the cutting force prediction. The effect of phase distortion due to the presence of time lag on the output prediction was studied. A performance index to characterize the phase distortion error was suggested for further improvement of untended machining.

1. Introduction

Today's technological innovations in manufacturing are driven by demands to maintain a consistent, high level of product quality in the modern manufacturing environment. At the same time, the ever increasing competition in the world market pushes the manufacturing industry to reduce production costs and to increase productivity. These challenges are forcing the manufacturing industry to consider untended machining as one of the major technical innovations to succeed in the modern manufacturing environment.

The effectiveness of utilizing untended machining has attracted great attention from the manufacturing industry. Its impact on the improvement of production automation and machining accuracy are evident. Under untended machining, the operator is not in a position to sense the operation. To replace the operator, an on-line monitoring system is used to ensure the product quality. It is expected that the on-line system, as an integral part, is built in the machine tool. Consequently, the success of an untended machining system is entirely dependent on the methods to perform sensing and control during machining. During the past 30 decades, various sensors, based on force, torque, power, vibration, acoustic emission, and vision, have been developed. Many of them have been successfully applied in monitoring the machining process. The availability of sophisticated computers further enables us to incorporate signature analysis techniques into untended

machining for the control of machining processes. The adaptive control system reported in [1] was used in a CNC milling machine. A dynamometer was attached to the spindle. Its on-line monitoring of the milling operation was through the detection of cutting force. A control algorithm was developed to adjust the table movements for keeping the dynamic variation of the cutting force within a preset level. It was reported in [2] that chipping of the cutting tool during machining was detected through an on-line monitoring of cutting force. The detected cutting force at each sampling instant was used as an input to a discreet autoregressive model that estimated the status of tool wear during machining. A common characteristic in the previous approaches is that the sensors were attached to the machine tool and were not built in the machine tool. Consequently, these researchers performed the calibration process, which is a complex undertaking, on their own. It is felt that the complexity involved in the calibration process and in the determination of monitoring strategy has slowed down the wide acceptance of untended machining significantly.

There has been a deterministic trend that a new generation of machine tools should be built to carry out untended machining. In these machine tools, sensors are built to function as an integral part for the on-line monitoring of various aspects of machining such as tool wear, tool breakage, material handling, and in-process inspection. It can be expected that the success of building these machine tools is heavily dependent on the availability and capability of the built-in sensors, or the built-in monitoring system. One of the major issues involved in designing the monitoring system is its calibration because the calibration data provides a basis for diagnostics of the machining process.

The work reported in this paper is the calibration of an on-line monitoring system built in a Matsuura CNC machining center. The on-line monitoring system mainly consists of a S2M magnetic bearing spindle with an Intel based data acquisition system and a control system [3-4]. During machining, the magnetic bearing spindle is subjected to the cutting force. The S2M control system reacts to the cutting force by varying the currents in the built-in electromagnetic coils to maintain the spindle in the center of its air gaps, both horizontally and vertically. To carry out a specific monitoring target such as tool wear, an indirect model-based method is used [5-6]. Through the detection of the cutting force variation, the tool wear progress during machining is retraced. we need to know the dynamic variation of the cutting force present during machining. Therefore, the calibration between the cutting force and the coil currents, or the air gaps, or both forms a basis for the establishment of a quantitative mapping function between them.

In section 2 of this paper, calibration under static loading is presented. The transformation matrix method used to establish the transfer function between the coil currents and the cutting force is discussed. Section 3 presents calibration under dynamic loading to characterize the dynamics of the magnetic bearing spindle in relation to the coil current variation. The integration of the two calibration processes forms a systematic approach to perform the calibration of an untended machining system.

2. Calibration under Static Loading

2.1 Description of the Equipment for Untended Machining

In order to carry out an intended machining process, a Matsuura 500 Vertical Machining Center was retrofitted with an S2M magnetic bearing spindle in place of the conventional spindle [3]. The basic structure of the S2M spindle is shown in Fig. 1. There are two sets of magnetic bearing coils located in two horizontal planes and one set in the vertical axis. When electrical currents flow through these coils, the generated magnetic forces maintain a uniform air gap around the spindle. During machining, the magnetic spindle is subjected to the generated cutting force. As a result, the air gap becomes uneven. At the same time, the position sensors, which are shown in Fig. 1, detect such changes and send feedback signals to the controller. The controller adjusts the coil currents to recover the uniform air gap. This monitoring cycle provides the capability of performing an untended machining process.

2.2 Cutting Force Measurement

During an untended machining process, there is always a need to replace the cutting tool when it becomes worn. It has been known that direct measurements of tool wear seem difficult [5]. On the other hand, indirect and model-based measurement methods to retrace tool wear through the cutting force measurement seem promising [6-9]. It has been reported that the thrust force acting on the drill during machining is a good indication for drill replacement [9]. Therefore, it is imperative to study the relation between the cutting force, such as the thrust force, and the coil currents in order to carry out the untended drilling process on the retrofitted CNC machining center. The necessity to calibrate this relation can also be felt when machining composite/steel laminate materials. An on-line adjustment for feedrate and spindle speed during machining is needed when the drill reaches the boundary between the composite and steel materials. A reliable signal to actuate this adjustment would be again the thrust force.

2.3 Calibration under Static Loading

Since the magnetic bearing spindle functions as a sensing system, it is a common practice to apply a known and static force at the end of the spindle during the calibration process. When the force is applied, the corresponding changes in the coil currents are recorded. By increasing, or decreasing, the applied force, the relationship between the applied force and the coil currents, or the transfer function of the sensing system, can be established [10].

It should be pointed out that the cutting force generated during machining is a vector in the three-dimensional space. The cutting force acts on the spindle. Consequently, there exist reaction forces at the bearing locations. As indicated in Fig. 2, the two reaction forces at the two radial bearings balance the two components of the cutting force acting in the horizontal plane (x-y plane), i.e., F_x and F_y . From the modeling viewpoint, each of the two reaction forces can be treated as a sum of two components, namely, the pair of F_{1x} and F_{1y}, or the pair of F_{2x} and F_{2y}. In the vertical plane, the reaction force at the thrust bearing balances the vertical component of the cutting force, F_z. Therefore, the calibration process requires analysis of the force transmission and establishment of the transfer functions between the applied force and the coil currents. In general, the calibration process consists of the following four steps.

Step 1: Transfer the cutting force, or the applied calibration force, into the five (5) components of the reaction forces at the three bearing locations. This means that the applied force is first decomposed into its three components, i.e., F_x, F_y, and F_z. Then, the three components are transferred into F_{1x}, F_{1y}, F_{2x}, F_{2y}, and F_z.

$$\begin{bmatrix} F_{1x} \\ F_{1y} \\ F_{2x} \\ F_{2y} \\ F_z \end{bmatrix} = \frac{1}{d_3} \begin{bmatrix} (d_2) & 0 & 0 \\ 0 & (d_2) & 0 \\ -(d_1) & 0 & 0 \\ 0 & -(d_1) & 0 \\ 0 & 0 & d_3 \end{bmatrix} \begin{bmatrix} F_x \\ F_y \\ F_z \end{bmatrix} \qquad (1)$$

where d_1 and d_2 are distances between the applied force and the two radial bearings, and d_3 is the distance between the two radial bearings. They are shown in Fig. 2.

Step 2: Identify the transfer function between the corresponding coil current and the reaction force component for each of the five pairs, i.e.,

$$
\begin{aligned}
TF_{1x} &= \frac{(\text{Coil Current})_{1x}}{(\text{Applied Force})_{1x}} = \frac{I_{1x}}{F_{1x}} \\
TF_{1y} &= \frac{(\text{Coil Current})_{1y}}{(\text{Applied Force})_{1y}} = \frac{I_{1y}}{F_{1y}} \\
TF_{2x} &= \frac{(\text{Coil Current})_{2x}}{(\text{Applied Force})_{2x}} = \frac{I_{2x}}{F_{2x}} \\
TF_{2y} &= \frac{(\text{Coil Current})_{2y}}{(\text{Applied Force})_{2y}} = \frac{I_{2y}}{F_{2y}} \\
TF_{z} &= \frac{(\text{Coil Current})_{z}}{(\text{Applied Force})_{z}} = \frac{I_{z}}{F_{z}}
\end{aligned}
\tag{2}
$$

Step 3: Assemble the five identified transfer functions into a transformation matrix. The transformation matrix is a diagonal matrix, assuming that there does not exist any cross-talking among the coil currents when subjected to the cutting force.

$$
[\,TF\,] = \begin{bmatrix}
TF_{1x} & 0 & 0 & 0 & 0 \\
0 & TF_{1y} & 0 & 0 & 0 \\
0 & 0 & TF_{2x} & 0 & 0 \\
0 & 0 & 0 & TF_{2y} & 0 \\
0 & 0 & 0 & 0 & TF_{z}
\end{bmatrix}
\tag{3}
$$

Step 4: Combine Eqs. (1), (2), and (3) to derive the mapping function between the cutting force components and the coil currents. The mapping function in a matrix form is given below.

$$
\begin{bmatrix} I_{1x} \\ I_{1y} \\ I_{2x} \\ I_{2y} \\ I_{z.} \end{bmatrix} = \begin{bmatrix}
TF_{1x} & 0 & 0 & 0 & 0 \\
0 & TF_{1y} & 0 & 0 & 0 \\
0 & 0 & TF_{2x} & 0 & 0 \\
0 & 0 & 0 & TF_{2y} & 0 \\
0 & 0 & 0 & 0 & TF_{z}
\end{bmatrix} \begin{bmatrix}
\frac{d_2}{d_3} & 0 & 0 \\
0 & \frac{d_2}{d_3} & 0 \\
\frac{-d_1}{d_3} & 0 & 0 \\
0 & \frac{-d_1}{d_3} & 0 \\
0 & 0 & 1
\end{bmatrix} \begin{bmatrix} F_x \\ F_y \\ F_z \end{bmatrix}
\tag{4}
$$

In the present work, the calibration process was carried out in three separate directions. For example, when the applied force is oriented in the x direction, the force

vector is equivalent to $[\,F_x \;\; 0 \;\; 0\,]^T$. This enables us to estimate TF_{1x} and TF_{2x}. Using the relation indicated in Eq. (1), we identify the two reaction forces in the x-direction, i.e., F_{1x} and F_{2x}. It has been observed that, among the five magnetic coils, only two magnetic coils respond to the applied force acting in the x-direction. Through the recording of the two coil currents, i.e., I_{1x} and I_{2x}, the two transfer functions can be established by the two ratios, $TF_{1x} = \frac{I_{1x}}{F_{1x}}$ and $TF_{2x} = \frac{I_{2x}}{F_{2x}}$ where I_{1x} and I_{2x} are the recorded coil currents during the calibration. Figure 1 illustrates the experimental setup of static loading to identify the five diagonal elements in the transformation matrix. During the calibration process, known weights were gradually added, from 10 Newtons to 510 Newtons with an interval of 50 Newtons in the x direction. The current changes in the five coils were recorded. Linear relations between the applied force and the coil currents were observed. The solid line shown in Fig. 3 is the plot of the applied force in the x direction F_x .vs. the coil current I_{1x}. Consequently, the slope of the line through regression analysis characterizes the transfer function $TF_{1x} = \frac{\Delta I_{1x}}{\Delta F_{1x}}$. In a similar manner, we estimate TF_{1y} and TF_{2y} when applying the static loading in the y direction, and estimate TF_z when applying the static loading in the z direction.

During machining, the detected signals from the on-line monitoring are the five coil currents. The corresponding three cutting force components can be known from the following matrix multiplication.

$$\begin{bmatrix} F_x \\ F_y \\ F_z \end{bmatrix} = \begin{bmatrix} 1 & 0 & -1 & 0 & 0 \\ 0 & 1 & 0 & -1 & 0 \\ 0 & 0 & 0 & 0 & 1 \end{bmatrix} \begin{bmatrix} \frac{1}{TF_{1x}} & 0 & 0 & 0 & 0 \\ 0 & \frac{1}{TF_{1y}} & 0 & 0 & 0 \\ 0 & 0 & \frac{1}{TF_{2x}} & 0 & 0 \\ 0 & 0 & 0 & \frac{1}{TF_{2y}} & 0 \\ 0 & 0 & 0 & 0 & \frac{1}{TF_z} \end{bmatrix} \begin{bmatrix} I_{1x} \\ I_{1y} \\ I_{2x} \\ I_{2y} \\ I_{z.} \end{bmatrix} \tag{5}$$

It is worth noting that special cares have been taken during the calibration under static loading. First, a mechanical ball bearing was attached to the end of the magnetic spindle, as shown in Fig. 1. The calibration force was directly applied to the mechanical ball bearing, then transmitted to the spindle. This attachment allowed the calibration

process to be carried out while the spindle was rotating in order to more closely mimic the machining environment. Second, the calibration process was duplicated at five different spindle speeds to study possible effects of the spindle speed on the transformation matrix. Among the five calibration data sets, three were plotted in Fig. 3. They represent the three calibration processes where the spindle speeds were set at 1000 rpm, 3000 rpm, and 5000 rpm, respectively. Examining the data shown in Fig. 3, there appears to be only a single straight line due to the fact that the estimated slope and intercept of each of the three calibration lines are so closed to each other. The difference among them can be hardly displayed by the scale used in Fig. 3. Although the three lines are not exactly collinear, using the calibration line at spindle speed setting 1000 rpm for other spindle speed settings can be justified from the statistical point of view. Consequently, this observation could justify using one transformation matrix when the spindle is under operation from 1000 rpm to 5000 rpm.

3. Calibration under Dynamic Loading

The need to perform a calibration under dynamic loading comes from the need to identify patterns of the dynamic variation of the cutting force. It has been reported that methods of using pattern recognition in the frequency domain are effective in detecting the tool wear progress during machining [9]. In order to perform the dynamic analysis of the cutting force variation in the frequency domain, and detect the dynamic variation of the cutting force during machining , the calibration process was also carried out under dynamic loading. The concern for calibrating the magnetic bearing spindle dynamically arises from the observation from previous research [8] that tool wear can be detected by monitoring the frequency components of the cutting force.

The calibration under dynamic loading consists of three parts, namely, the impulse response test, the frequency response test, and the phase distortion test. Each test is designed to perform specific tasks, such as identification of natural frequency, damping coefficient, gain factor, and phase shift. An integration of these test results presents a comprehensive description of the system dynamics of the magnetic bearing spindle in the frequency domain.

The impulse response test was used to determine the natural frequency and the damping ratio of the magnetic bearings. Figure 4 is the plot of the response of the magnetic bearing spindle to impulsive loading. The response pattern shown in Fig. 4 strongly suggests that the dynamic characteristics of the magnetic bearing spindle can be modeled as

a second-order system. The recorded time interval for a single cycle is approximately equal to 0.008 second. The natural frequency of the magnetic bearing spindle is estimated to be 125 Hz. The damping coefficient, equal to 0.13, is also estimated from the decay envelope.

To perform the frequency response test, a HP Digital signal analyzer and a shaker amplifier were used. The experimental setup is illustrated in Fig. 5. The signal analyzer injected white noise into the shaker amplifier to generate an excitation characterized with a flat frequency spectrum. Figure 6 presents the Bode plot from the signal analyzer. The response pattern is typical of a second-order system when subjected to white noise excitation. At the low frequency range from 0 Hz to 80 Hz, the gain factor is almost kept at a unity (db) level. At the high frequency range, the gain factor decreases as the excitation frequency increases. At the frequency range between 80 Hz and 200 Hz, the gain factor changes dramatically, indicating that the excitation frequency is closed to the natural frequency of the magnetic bearing spindle. As shown in Fig. 6a, the resonance frequency is about 125 Hz, which matches the experimental results obtained during the impulse response test. These observations confirm the validity of using a second order model to predict the response of the magnetic bearing spindle in the frequency domain. Examining the Bode plot carefully, the gain factor remains close to unity between 0 and 80 Hz. The gain factor increases significantly when the excitation frequency approaches 125 Hz. Figure 6b is the phase shift plot. It indicates that the phase shift is relatively constant between 0 and 80 Hz. The phase shift angle is about 12.5^{o}. This shift angle indicates that the response of the magnetic bearing spindle, or the dynamic variations of the coil currents, lag behind the dynamic variation of the cutting force during machining. The time lag is given by the phase shift angle divided by the angular frequency $2\pi f$ [11]. It is evident that the time lag in the frequency range from 0 to 80 Hz varies and decreases as the excitation frequency increases. Consequently, the dynamic variation of the coil currents may not give an accurate picture of the dynamic variation of the cutting force during machining. This indicates that the distortion in the wave form of the applied force with respect to the recorded wave form of the coil currents is likely to occur.

In order to verify just how faithfully the magnetic bearing spindle sensing system will be recording the dynamic cutting force during machining, the phase distortion test was designed to quantify the time lag under different excitation frequencies [11]. When the time lag is known, the difference between the recorded coil currents and the actual cutting forces can be evaluated. The actual cutting force can be recovered from the recorded coil currents. Figure 7 shows the experimental set up used. Two function generators were connected in

parallel to the shaker amplifier. They excited the shaker with sinusoidal waves of two specified and different frequencies. As a result, the excitation force generated by the shaker amplifier consisted of two frequency components. It was expected that the recorded coil currents also contained the same frequency components. During the test, the excitation force acting on the spindle and the resulting coil current signals were recorded by an Haitachi 20 MHz digital storage oscilloscope, and down loaded into an IBM/AT. The input and output wave forms were then compared in the time domain. Figure 8 shows the input wave as a dotted curve and the output wave as a solid curve. The excitation frequencies were 10 Hz and 30 Hz. The time lag between the input and output was measured through a shifting process to mate the two patterns. As illustrated in Fig. 8a, the time lag is 10.5 ms. After shifting the output curve to the left for mating the input pattern, the areas between the two curves shown in Fig. 8b reflects the distortion between the input and output.

4. Discussion of Results

4.1 A Case Study: On-Line Monitoring of Tool Wear

In order to demonstrate the on-line monitoring of tool wear during machining, a prototype system was developed using an indirect model-based method. We assumed that the magnitude of the cutting force would increase as tool wear progressed. In addition, a sudden drop in the magnitude of the cutting force would also indicate the occurrence of tool breakage. Therefore, as long as the magnitude of the cutting force varied within two preset limits during the monitoring, the machining process should continue on. Otherwise, human intervention should be called in.

Because of the availability of the transformation matrix through the calibration process, the monitoring of tool wear can be performed through the on-line detection of the coil currents. The machining process was to mill slots in a composite material. The end mill diameter was 12.7 mm. The cutting parameters were set at spindle speed = 1000 rpm, feedrate = 60 mm/min, and depth of cut = 4 mm. Table 1 is a list of the measured coil currents in a consecutive time order. The three predicted cutting force components are calculated using the calibrated transformation matrix. As an example, the three cutting force components listed in row 1 were calculated using Eq. (4).

$$\begin{bmatrix} 3.04 \\ 74.58 \\ 92.4 \end{bmatrix} = (4.45) \begin{bmatrix} 1 & 0 & -1 & 0 & 0 \\ 0 & 1 & 0 & -1 & 0 \\ 0 & 0 & 0 & 0 & 1 \end{bmatrix} \begin{bmatrix} 92.4 & 0 & 0 & 0 & 0 \\ 0 & 99.66 & 0 & 0 & 0 \\ 0 & 0 & 158 & 0 & 0 \\ 0 & 0 & 0 & 151 & 0 \\ 0 & 0 & 0 & 0 & 86.5 \end{bmatrix} \begin{bmatrix} .11 \\ -.15 \\ .06 \\ -.21 \\ .24 \end{bmatrix}$$

Figure 9 was the control chart designed for monitoring the thrust force acting on the end mill. The center line of the control chart was determined by the mean value, -65.12 Newtons, calculated from the 15 detected thrust forces (note: the time period should be longer for calculating this mean value in a practical application). The upper and lower control limits were established using the $\pm 3\sigma$ principle where parameter σ stands for the standard deviation of the thrust force about its mean level and is equal to 229 Newtons calculated from the 15 detected thrust forces. The decision-making policy was that the milling should be stopped when the on-line detected thrust force(s) beyond the upper limit, or below the lower limit.

4.2 Evaluation of Phase Distortion Effect

For an accurate monitoring of the cutting force during machining, it would be desirable to quantitatively evaluate the effect of the phase distortion on the cutting force prediction, and, if possible, to compensate the error for the recovery of the true cutting force signal. A performance index to characterize the phase distortion error was developed in this research. As shown in Fig. 8a, the displayed input and output signals were recorded directly from the oscilloscope during the phase distortion test. In Fig. 8b, the output signal was shifted to the left to match the input signal pattern. The shifted distance represents the time lag, which indicates that the dynamic variation of the measured coil currents lags behind the excitation force. By integrating the two curves to get the two covered areas and subtracting the two areas, a quantitative measure of the phase distortion error can be obtained. For comparison, the evaluated difference was normalized with respect to the time period used during the integration process. The normalized difference was used as the performance index to characterize the phase shift effect. The larger the difference, the greater the phase shift error. Several calculated normalized difference is listed below.

Combination of Frequencies	5 & 6	10 & 30	50 & 55
Normalized Difference	0.1	28.5	0.2

Examining the listed values, it is evident that the normalized difference increases as the difference between the two combined frequencies. The research is going on at the University of Maryland, is to compensate the phase distortion error to recover the true cutting force signal for further improvement of on-line monitoring.

V. Conclusions

1. A CNC machining center equipped with a magnetic bearing spindle was used as a test bed to perform untended machining. In order to monitor the dynamic variation of the cutting force during machining, a strategy of measuring the coil currents in the magnetic bearings was used. The dynamic variation of the cutting force was being indirectly monitored through the detection of the coil current variation. A calibration procedure was developed to establish the relationship between the three components of the cutting force and the coil currents for the purpose of performing untended machining.

2. Calibration under static loading was carried out to identify the transfer function between the statically applied force and the coil currents. The matrix transformation method was used. The force decomposition matrix establishes the relationship between the applied force and the reaction force on each of the magnetic bearing locations. The mapping function matrix establishes the relationship between the reaction forces and the coil currents. Combination of these two matrices leads to the identification of the system transfer function under static loading.

3. Calibration under dynamic loading identified the dynamic characteristics of the coil current variation in relation to the dynamic characteristics of the magnetic bearing spindle. It has been found that system dynamics of the magnetic bearing spindle can be represented by a second order system with a natural frequency equal to 125 Hz and a damping coefficient equal to 0.13. The most significant finding is the distortion in the wave form of the applied force with respect to the recorded wave form of the coil currents. Time lags were experimentally determined to quantify the effect of phase distortion on the prediction accuracy of the cutting force through the measurements of the coil currents.

4. As a demonstration example, a prototype system to perform an on-line monitoring of the tool wear progress was presented. Using the indirect model-based method, the coil currents were detected during machining to predict the cutting force, which retraced the tool wear status during machining. A system performance index, called normalized phase distortion error, was developed to characterize the phase distortion effect on the prediction accuracy, showing good promise for further improvement of monitoring sensitivity.

Acknowledgements

The authors acknowledge the support of the Systems Research Center at the University of Maryland at College Park under Engineering Research Centers Program: NSFD CDF 8803012. They also express their gratitude to the College of Engineering for the financial support through Minta Martin funding. They wish to thank Dr. M. Abdulhamid for his technical support in this research.

References

1. J. Tlusty, A. Cowley, M. Elbestawi, "A Study of an Adaptive Control System for Milling with Force Constraint",Sixth NAMRC Proceedings, Society of Manufacturing Engineers, 1978, pp. 364-371.

2. M. Lan, Y. Naerheim, "In-Process Detection of Tool Breakage in Milling", Sensors and Controls for Manufacturing, ASME, San Fransico, CA, November 17-22, 1985, pp. 49-56.

3. E. Zivi, Robust Control of a Magnetic Bearing Spindle for Increased Milling Tool Accuracy. Ph. D. Dissertation, University of Maryland, 1989

4. E.L. Zivi, D.K. Anand, M. Anjanappa, and J.A. Kirk, "Magnetic Bearing Spindle Control for Accuracy Enhancement in Machining," 1990 ASME Winter Annual Meeting, Dallas, Texas, November 1990.

5. Y. Koren, T. Ko, K. Danai, and A. Ulsoy, "Methods for Tool Wear Estimation from Force Measurements Under Varying Cutting Conditions", Control Issues in Manufacturing Processes, ASME, Miami Beach, FL, December 10-15, 1989, pp.45-53.

6. K. Danai and A. Ulsoy, "An Adaptive Observer for On-Line Tool Wear Estimation in Turning, Part I and II," Mechanical System and Signal Processing, 1987, pp. 211-240.

7. G. Chryssolouris, M. Guillot, and M. Domroese, "Tool Wear Estimation for Intelligent Machining", Intelligent Control, ASME, Boston, MA, December 13-18, 1987. pp.35-43.

8. J.-J, Park, and A. G. Ulsoy, "On-Line Tool Wear Estimation Using Force Measurement and a Nonlinear Observer", Control Issues in Manufacturing Processes, ASME, Miami Beach, FL, December 10-15, 1989, pp.55-63.

9. P. Bandyopadhyay, and S. M. Wu, "Signature Analysis of Drilling Dynamics for On-Line Drill Life Monitoring", Sensors and Controls for Manufacturing, ASME, San Fransico, CA, November 17-22, 1985, pp.101-110.

10. G. M. Zhang and S. G. Kapoor, "Development of An Instrumented Boring Bar Transducer," The 14th North American Manufacturing Research Conference Proceedings, pp. 194-200, May 1986.

11. S. S. Rao, Mechanical Vibrations, second edition, Addison Wesley, 1990, pp. 501-502.

List of Tables

List of Figures

Current Measered at Bearings (Volts)

Ix1	Iy1	Ix2	Iy2	Fz1
0.11	-0.15	0.06	-0.21	0.24
-0.03	-0.03	0.00	0.04	-0.13
0.00	-0.09	0.04	0.09	0.31
-0.04	0.02	0.07	-0.02	-0.02
0.05	0.01	-0.01	0.02	0.10
0.08	-0.01	-0.05	0.07	0.04
-0.05	0.01	-0.07	0.01	-0.28
0.04	-0.09	0.05	0.23	0.34
-0.06	0.03	-0.02	0.03	-0.30
-0.06	-0.05	0.12	0.05	0.14
0.01	0.02	-0.01	0.05	-0.58
0.00	0.02	-0.04	-0.02	0.31
0.07	-0.05	-0.04	0.06	1.37
-0.01	-0.04	-0.02	0.06	0.26
-0.05	-0.16	0.06	0.17	1.05

Calculated Cutting Forces (Newtons)

Fx	Fy	Fz
-0.48	-51.45	-90.44
11.52	-10.72	48.61
-19.25	-13.26	-118.63
-19.63	5.71	9.15
-10.17	-11.34	-39.70
3.17	-30.78	-17.15
51.18	-7.49	103.75
-35.45	-81.43	-129.90
28.32	-25.96	116.26
-40.66	-7.71	-52.86
2.19	-29.13	223.37
18.58	1.86	-118.63
-0.27	-13.89	-528.27
15.55	-13.09	-101.71
-13.36	-29.17	-404.25

Table 1: Measured Coil Currents and Predicted Cutting Forces

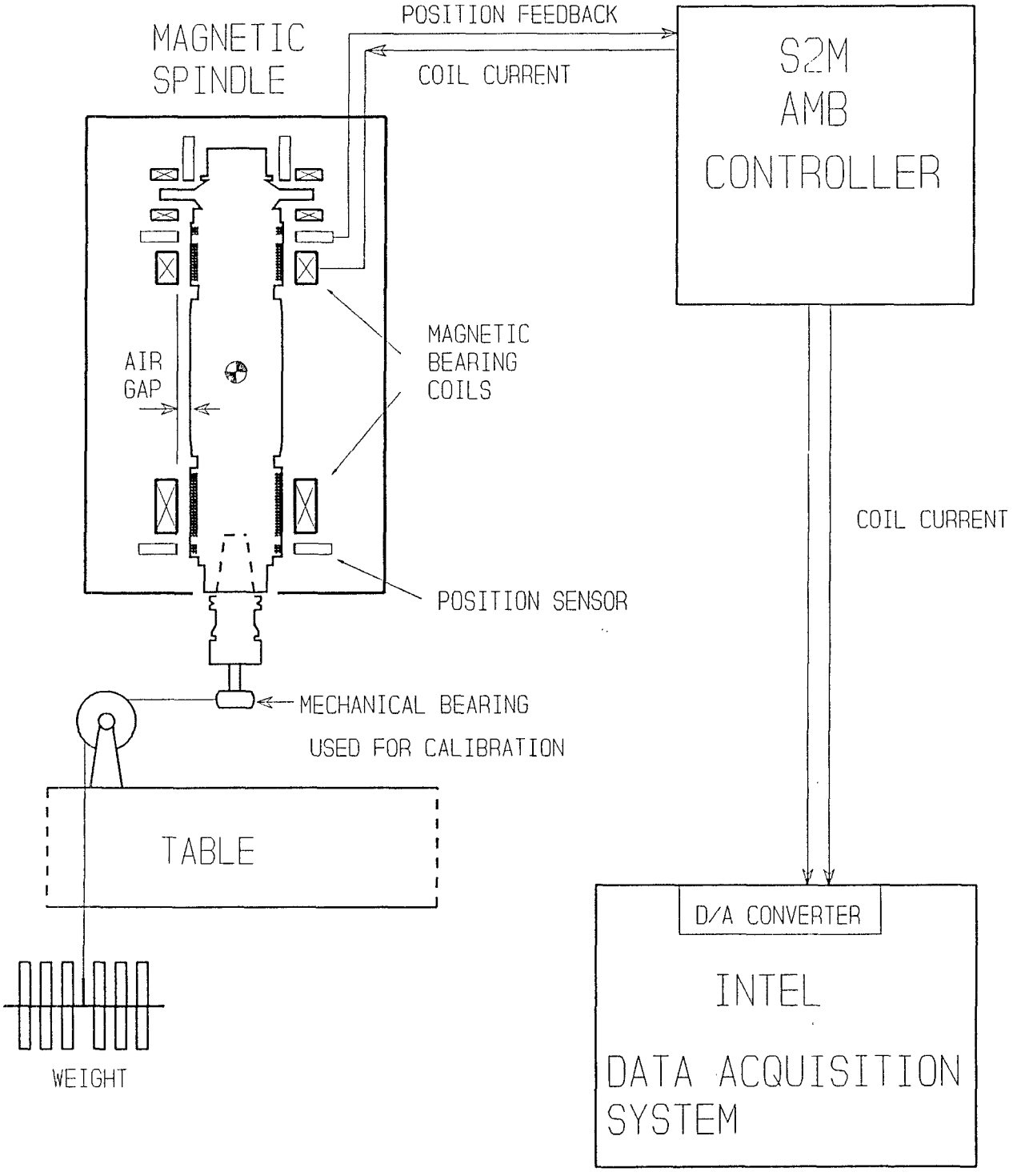

Figure 1: Matsuura 500 Machining Center with the S2M Magnetic Bearing Spindle and the Experimental Setup for Static Loading Calibration

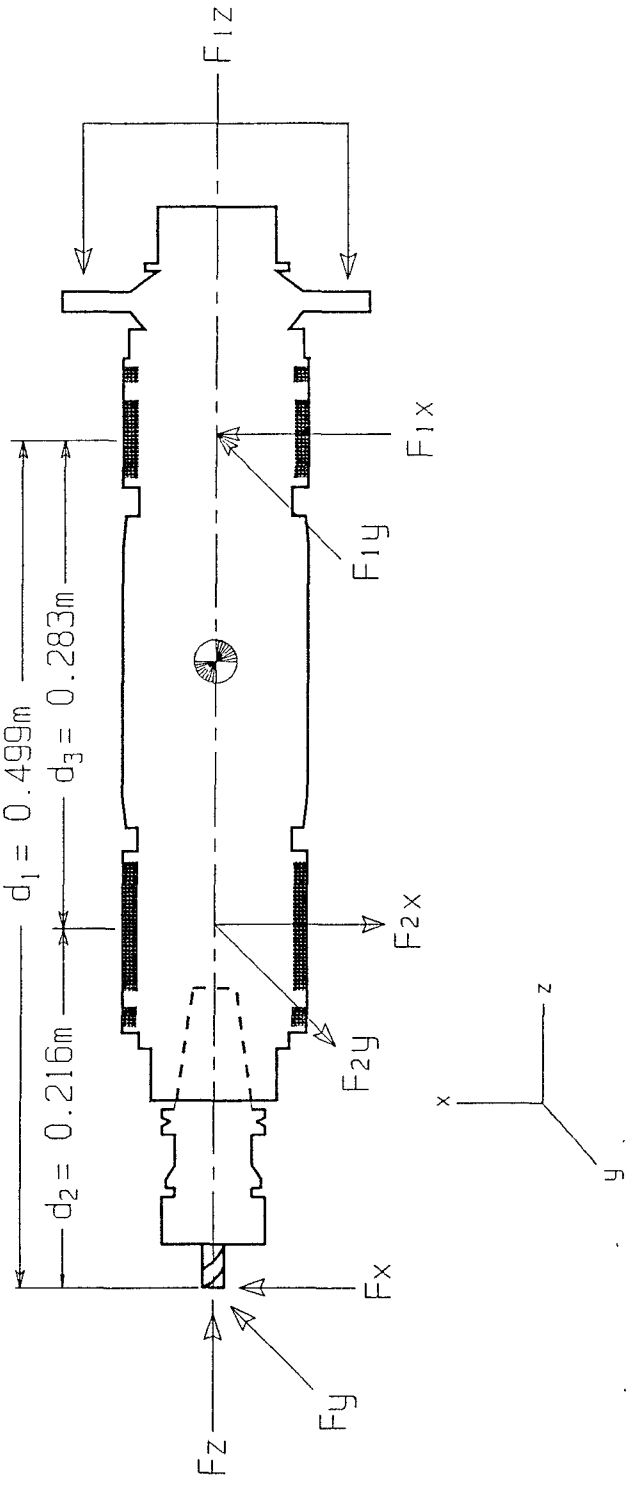

Figure 2: Decomposition of the Reaction Force
when Subjected to the Applied Loads

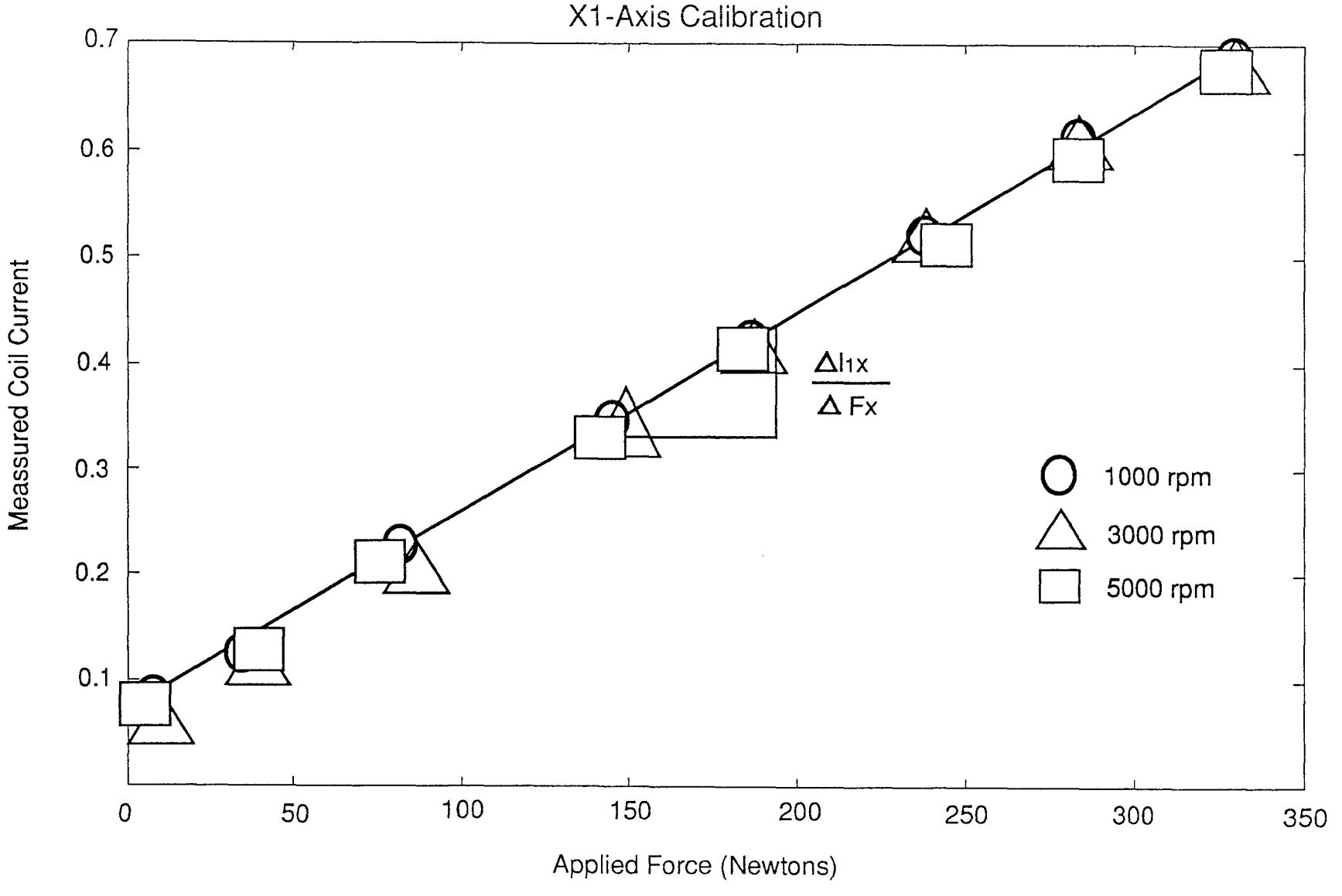

Figure 3: Calibration Plot to Illustrate the Determination of Transfer Function $\frac{I_{1x}}{F_{1x}}$

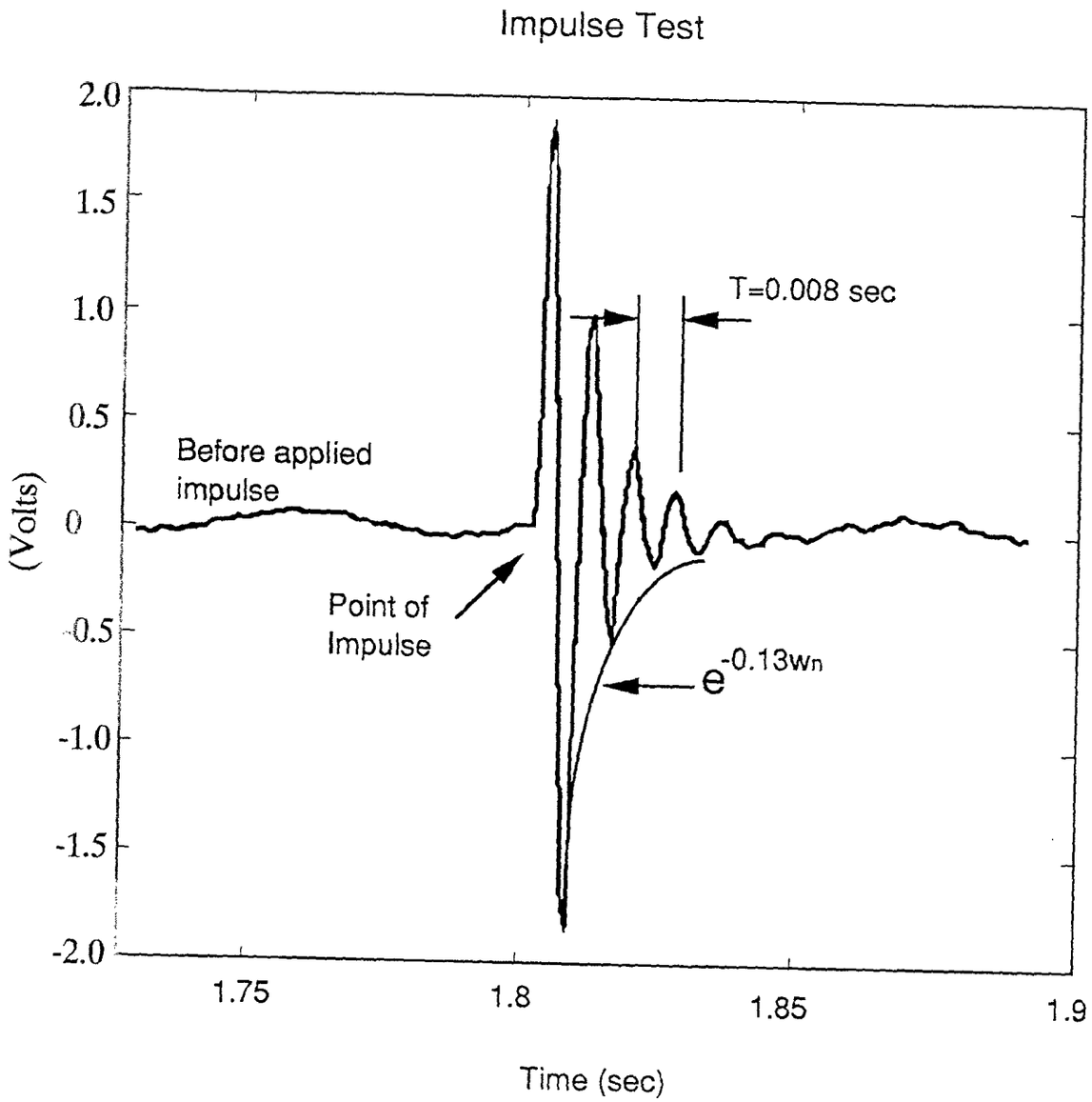

Figure 4: Experimental Data Recorded during the Impulse Test

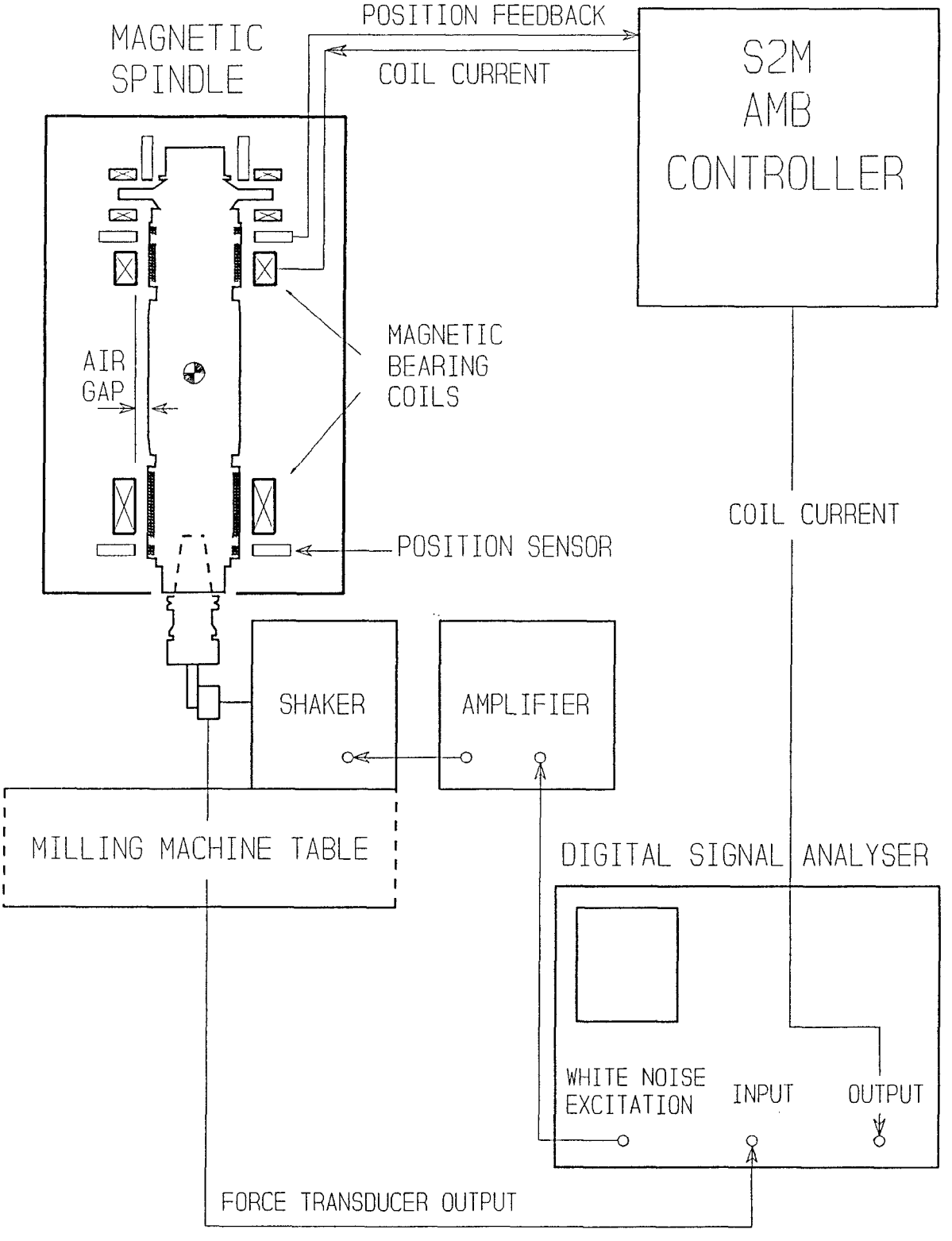

Figure 5: Experimental Setup for Dynamic Loading Calibration

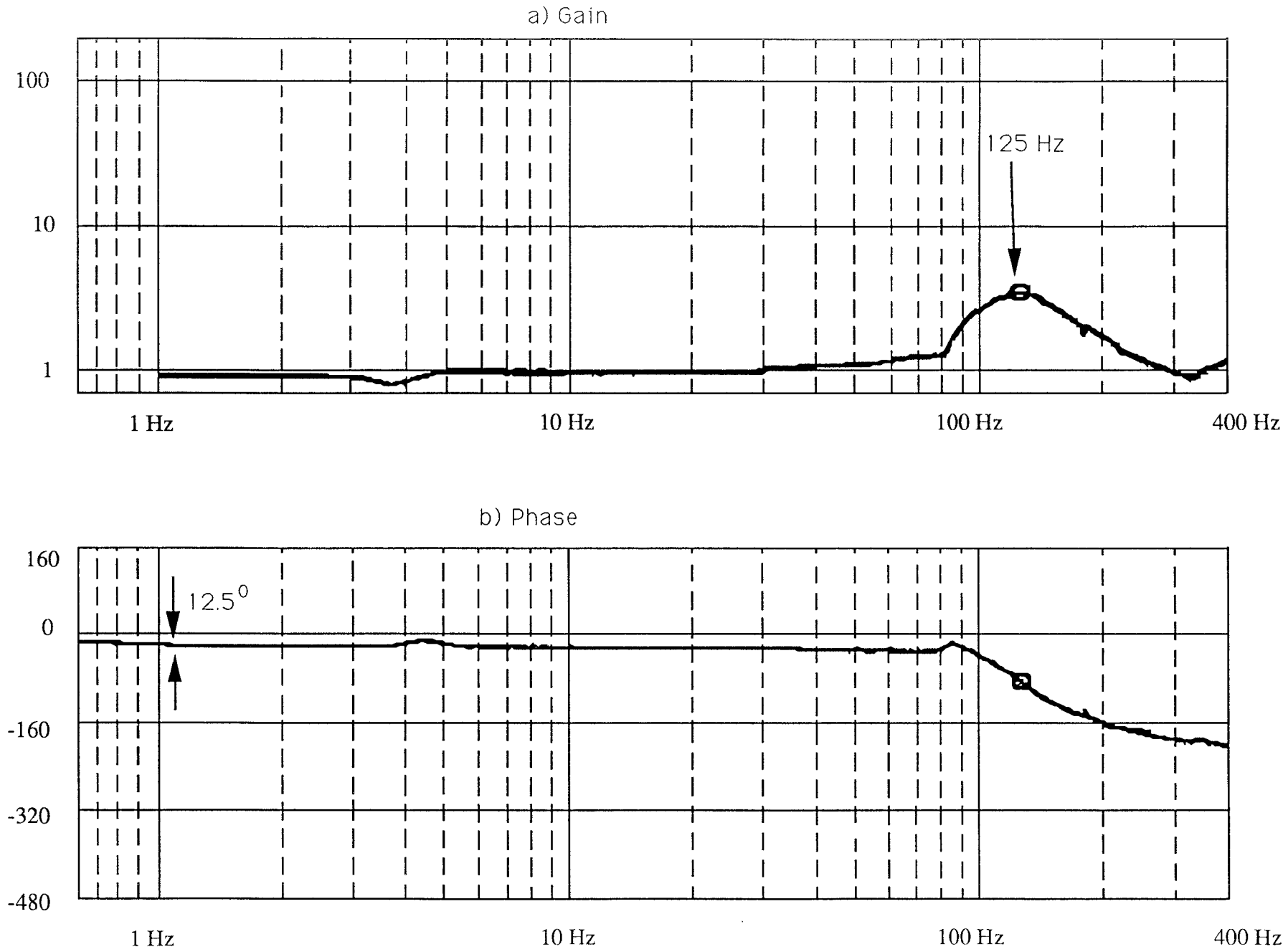

Figure 6: Plots of Amplitude and Phase Angle of the Coil Currents vs Excitation Frequency

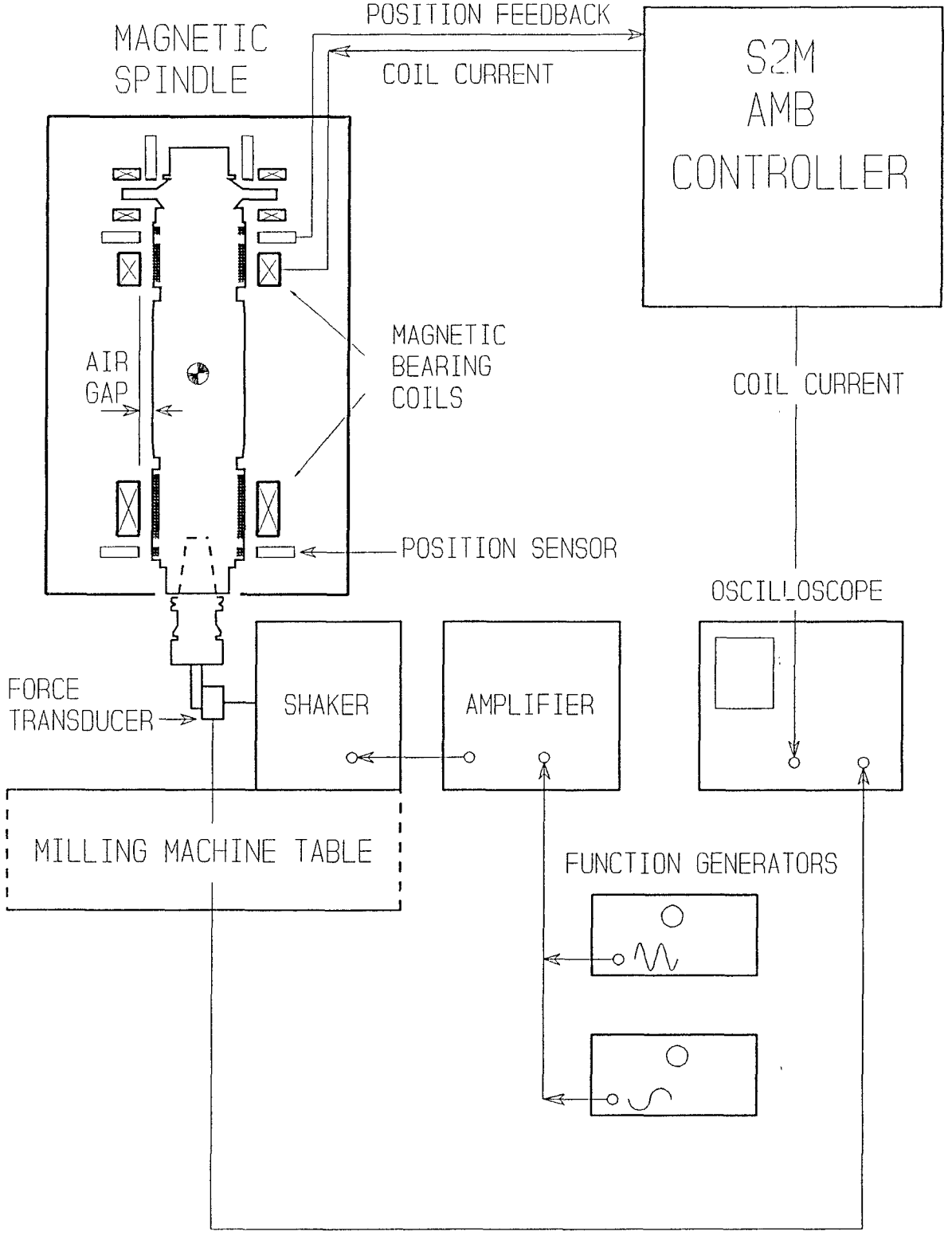

Figure 7: Experimental Setup for Testing Phase Distortion

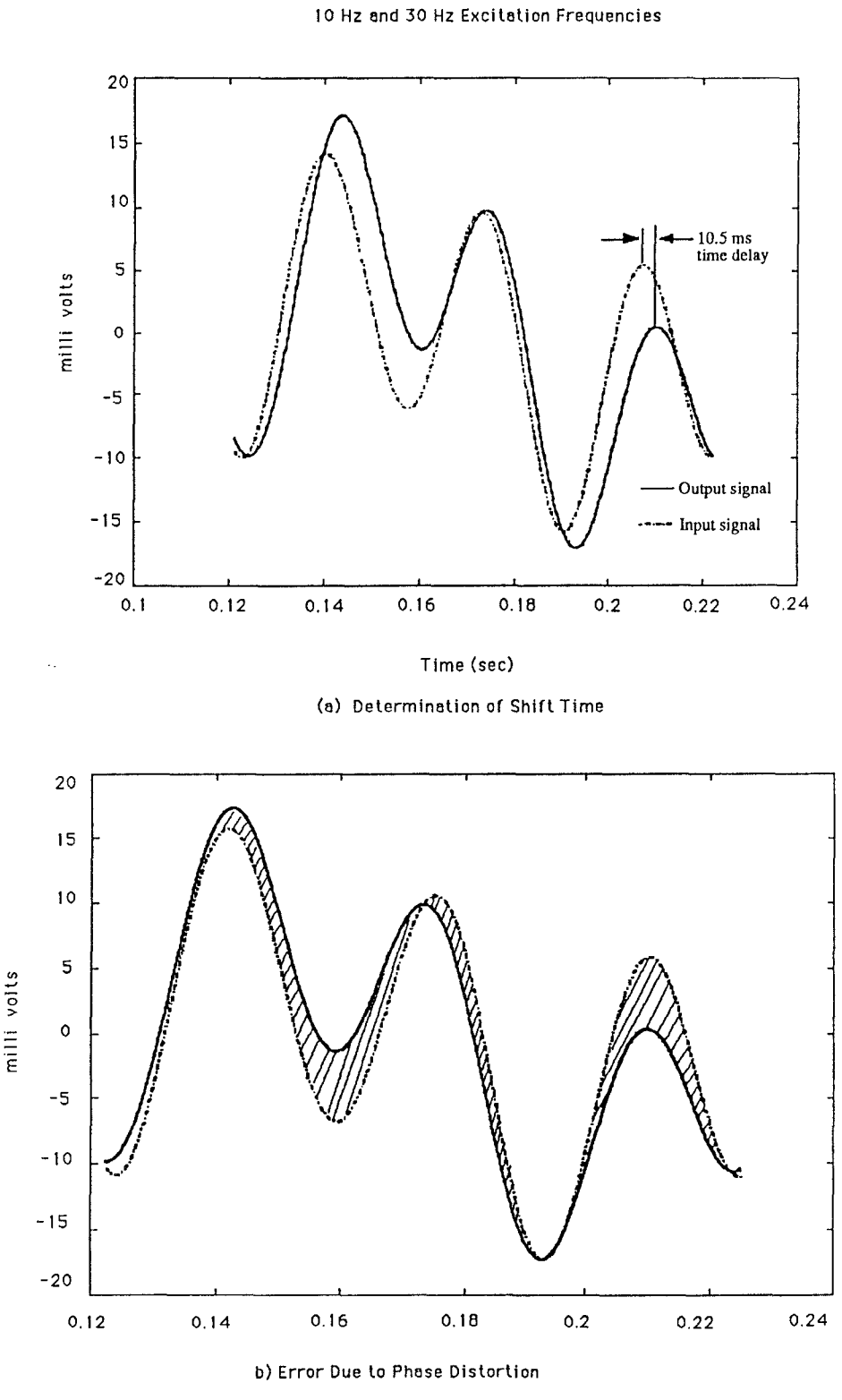

Figure 8: Shift of the Coil Current Response with Respect to the Excitation Signal Consisting of Two Frequencies (10 Hz and 30 Hz)

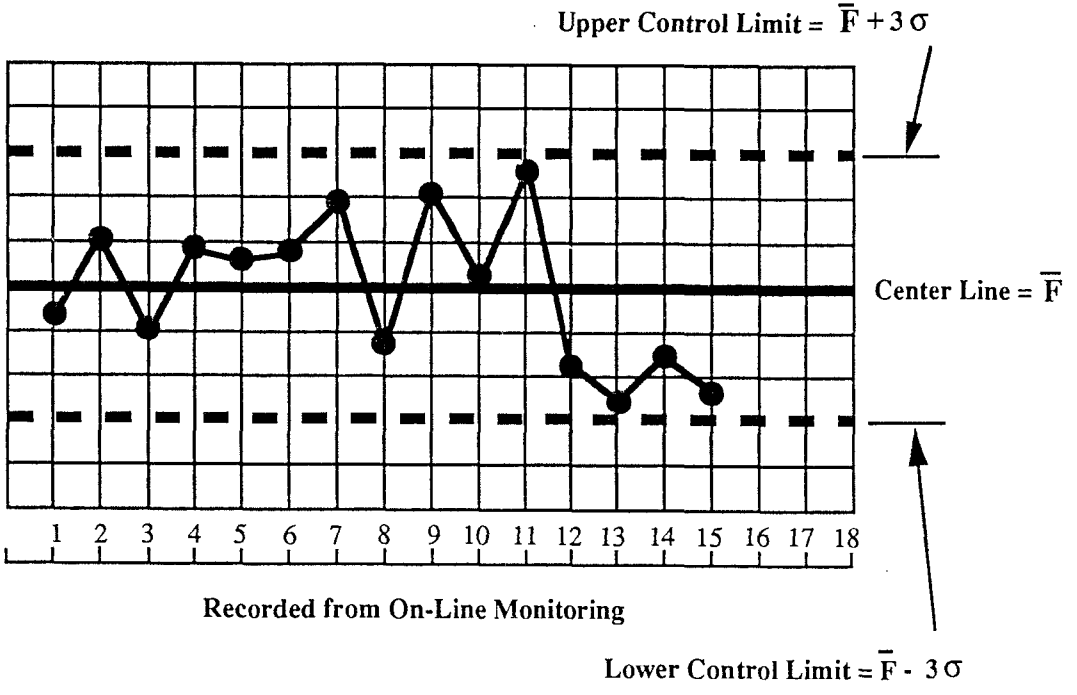

Figure 9: Control Chart Designed for Monitoring the Thrust Force during the Machining of a Composite Material